ChemComm

COMMUNICATION

View Article Online
View Journal | View Issue

Cite this: *Chem. Commun.*, 2014, **50**, 5590

Received 20th March 2014,
Accepted 3rd April 2014

DOI: 10.1039/c4cc02093f

www.rsc.org/chemcomm

Endoplasmic reticulum targeted chemotherapeutics: the remarkable photo-cytotoxicity of an oxovanadium(IV) vitamin-B6 complex in visible light†

Samya Banerjee,[a] Akanksha Dixit,[b] Radhika N. Shridharan,[b] Anjali A. Karande*[b] and Akhil R. Chakravarty*[a]

An oxovanadium(IV) vitamin-B6 Schiff base complex, *viz.* [VO(HL)-(acdppz)]Cl, having (acridinyl)dipyridophenazine (acdppz) shows specific localization to endoplasmic reticulum (ER) and remarkable apoptotic photocytotoxicity in visible light (400–700 nm) in HeLa and MCF-7 cancer cells (IC_{50} < 0.6 μM) while being non-toxic in the dark and to MCF-10A normal cells (IC_{50} > 40 μM).

Chemotherapy or photodynamic therapy (PDT) generally involves targeting nuclear or mitochondrial DNA, *e.g.* cisplatin as a nuclear DNA cross-linking agent and Photofrin® activity in mitochondria in PDT.[1–5] An alternate and hitherto less explored pathway is to achieve cellular apoptosis by targeting endoplasmic reticulum (ER) which plays crucial roles in the folding of proteins.[6–8] Any stress generated in the ER leads to ER stress response (ERSR) which could cause cell death *via* the intrinsic pathway of apoptosis involving the mitochondria. Thus, cell death by reactive oxygen species (ROS) triggered by ERSR could be a convenient way to treat different forms of tumours. Developing such tumour specific delivery agents to the ER could improve the efficacy of an anti-cancer agent by differentiating normal from the tumor cells, thereby reducing the undesirable side effects arising from the damage of any normal cells and eliminating the possibility of mutation of nuclear DNA. The delivery system generally consists of a tumour recognition moiety linked to a group which can generate ROS for desired cytotoxic or photocytotoxic response. With this objective we have designed a ternary oxovanadium(IV) complex of a Schiff base derived from vitamin B6 (VB6) and the dipyridophenazine derivative (acdppz) as the photosensitizer with an acridinyl fluorophore.[9] VB6 is known to be taken up by cells through a VB6 transporting membrane carrier (VTC) mediated diffusion pathway. As cancer cells have high demand for VB6, compounds having this moiety could achieve VTC mediated entry into the tumour cells in preference to the normal ones.[10] Herein, we report the unprecedented ER-targeted photocytotoxicity in visible light of a vitamin B6 Schiff base ($H_2L{\cdot}HCl$) oxovanadium(IV) complex [VO(HL)(acdppz)]Cl in HeLa and MCF-7 cancer cells while being essentially non-toxic to normal MCF-10A cells and in the dark (Fig. 1(a)).

Complexes [VO(HL)(B)]Cl (**1** and **2**), where B is 2,2′-bipyridine (bpy in **1**) and 11-(9-acridinyl)dipyrido[3,2-*a*:2′,3′-*c*]phenazine (acdppz in **2**), were synthesized in ~80% yield by reacting vanadyl chloride with the respective heterocyclic base and the Schiff base in ethanol.‡ The one-electron paramagnetic and 1 : 1 electrolytic VO^{2+} complexes showed a metal-centred visible band near 750 nm in 10% aqueous DMF and a broad band near 440 nm assignable to $PhO^- \rightarrow V^{IV}$ ligand-to-metal charge transfer (LMCT) transition.[5c] The acdppz ligand in **2** showed two additional bands near 362 and 390 nm assignable to the π–π* transition of the dppz and acridine chromophore, respectively (Fig. 1(b)).[9] The ESI-MS of the complexes showed essentially a single peak corresponding to $[M]^+$ in methanol (Fig. S1 and S2, ESI†). The complexes displayed IR peaks at ~955 cm^{-1} and ~1605 cm^{-1} for the V=O and the co-ordinated C=N stretching vibrations (Fig. S3, ESI†). Complex **2** showed green emission at 520 nm in 5% aqueous DMSO giving a quantum yield (ϕ) value of 0.05 when excited at 390 nm (Fig. 1(b)). The EPR spectrum of **2** at 25 °C in MeOH showed a typical isotropic eight-line resonance centered at g = 1.996 due to

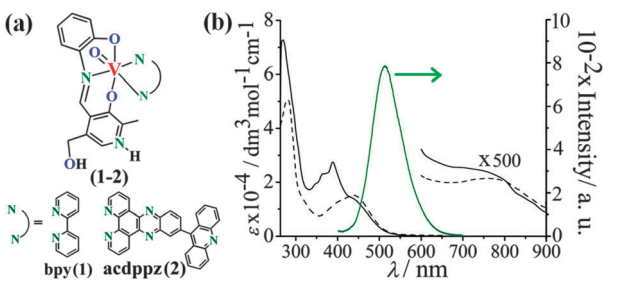

Fig. 1 (a) VO^{2+} complexes and the ligands used. (b) Absorption spectra of complexes **1** (- - -) and **2** (——) in 10% aq. DMF (black). Emission spectrum of complex **2** in 5% aq. DMSO (green) [$\lambda_{excitation}$ = 390 nm].

[a] *Department of Inorganic and Physical Chemistry, Indian Institute of Science, Bangalore 560012, India. E-mail: arc@ipc.iisc.ernet.in; Tel: +91-80-22932533*
[b] *Department of Biochemistry, Indian Institute of Science, Bangalore 560012, India. E-mail: anjali@biochem.iisc.ernet.in; Tel: +91-80-22932306*

† Electronic supplementary information (ESI) available: Synthesis, characterization, crystallography and cellular data (Fig. S1–S28, Tables S1–S3). CCDC 974426. For ESI and crystallographic data in CIF or other electronic format see DOI: 10.1039/c4cc02093f

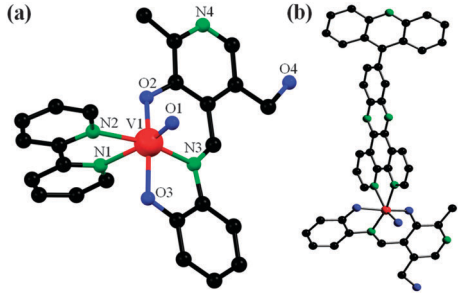

Fig. 2 (a) Structure of the complex in **1a**·EtOH. (b) Energy-optimized structure of **2**. Color codes: C, black; N, green; O, blue and V, red.

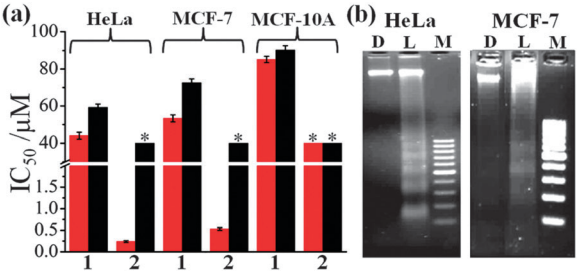

Fig. 3 (a) Photocytotoxicity of **1** and **2** from MTT assay in the cell lines upon 4 h incubation in the dark (black bar) and visible light (400–700 nm, red bar) [* for samples up to 40 μM concentration]. (b) DNA ladder of **2** in cancer cells showing apoptosis: D, dark; L, in light; M, Marker 100 bp.

hyperfine coupling of the ^{51}V nucleus (I = 7/2) (Fig. S4, ESI†). Cyclic voltammetry displayed an irreversible V(IV)/V(III) reduction near −0.9 V *vs.* S.C.E. in 20% DMF–H_2O with 0.1 M $[Bu^n_4N](ClO_4)$ (Fig. S5, ESI†). The complexes did not show any oxidative response. The redox stability of the VO^{2+} moiety is likely to reduce the dark cytotoxicity of the complexes. The complexes are stable in DMSO–Tris buffer and in 10% DMEM as evidenced from the UV-visible spectral studies showing no apparent spectral changes even after 48 h (Fig. S6, ESI†). Time-dependent mass spectral data also did not show any change in the spectral pattern up to 48 h (Fig. S1(b) and S2(b), ESI†). The complexes are photo-stable with no spectral change even after 6 h of photo-exposure (400–700 nm, Luzchem photo reactor, 10 J cm^{-2}) (Fig. S7, ESI†).

Complex **1**, as its perchlorate salt (**1a**), was structurally characterized (Fig. 2(a)). Complex **1a**·EtOH crystallized in the triclinic space group $P\bar{1}$ with two molecules in the unit cell. The complex has a distorted octahedral VO_3N_3 core with the *N*,*O*,*O*-donor Schiff base bonded to the VO^{2+} moiety in a meridional fashion and the *N*,*N*-donor bpy binds at the axial-equatorial sites of the VO^{2+} moiety (Table S1, Fig. S8 and S9, ESI†). The V=O distance is 1.598(2) Å. The V(1)–N(1) bond of 2.319(2) Å being *trans* to the V=O group is significantly longer than the other V–N bonds [2.134(2)–2.089(2) Å]. The V–O distances involving the Schiff-base are ∼1.970 Å. The O(2)–V(1)–O(3) angle is 157.83(9)°. The O(1)–V(1)–N(1) and N(3)–V(1)–N(2) angles show ∼16° deviation from the ideal *trans* disposition. There are H-bonding interactions between lattice ethanol and the complex. The pyridoxal NH is involved in H-bonding to the perchlorate anion (Fig. S10, ESI†). The DFT study showed the HOMO and LUMO to be concentrated over the Schiff base moiety in **1**.[11] The acridine moiety in **2** mostly contributes to the HOMO, while the LUMO is located over the Schiff base (Fig. 2(b), Fig. S11–S13, ESI†).

The photocytotoxic potential of the complexes was studied by 3-(4,5-dimethylthiazole-2-yl)-2,5-diphenyltetrazolium bromide (MTT) assay in human cervical carcinoma HeLa, human breast adenocarcinoma MCF-7 and breast epithelial MCF-10A cell lines (Table 1). The IC_{50} values of **2** are 0.24 ± 0.02 μM in HeLa cells and 0.53 ± 0.03 μM in MCF-7 cells in visible light (400–700 nm, Luzchem photo reactor, 10 J cm^{-2}), while being non-toxic in the dark (IC_{50} >40 μM) even after 48 h of incubation (Fig. 3(a), Fig. S14–S19, ESI†). Complex **1** in the absence of a photoactive moiety is not cytotoxic under light or dark conditions. Complex **2** showed no cytotoxic effect on MCF-10A, the normal counterpart of MCF-7 cells. The IC_{50} of **2** in the light increased to 8.7 μM upon pre-incubation with 4 mM vitamin-B6 indicating a VTC-mediated diffusion pathway likely to be operative for the cellular uptake (Fig. S19, ESI†). Complex **2** is remarkable in the chemistry of PDT showing photocytotoxicity at nanomolar concentration with low dark toxicity and excellent selectivity to the cancer cells over the normal cells. The photocytotoxicity of **2** in visible light is higher than its analogue [VO(cur)(dppz)Cl] (IC_{50} = 3.3 ± 0.4 μM) and comparable to that of Photofrin® (IC_{50} = 4.3 ± 0.2 μM in red light of 633 nm in HeLa cells and >41 μM in dark).[3a,12] DNA laddering performed with **2** to explore the mode of cell death showed ladder formation only upon light exposure to the cells, indicating apoptotic cell death, while no apparent cell death was observed in the dark (Fig. 3(b)). The Annexin-V/PI binding assay further confirmed apoptotic cell death. A 4 h incubation of the cells with complex **2** and subsequent photo-irradiation for 1 h showed ∼35% early apoptosis in the cancer cells (Fig. S20 and S21, ESI†). We probed for ROS formation from DCFDA (2′,7′-dichlorofluorescein diacetate) assay in HeLa cells. Complex **2** forms ROS only upon exposure to light (Fig. S22, ESI†). Further study showed formation of $^1O_2$ as the ROS with ϕ = 0.22(±0.02) in methanol.

The cellular internalization of complex **2** was studied by FACS analysis (Fig. S23, ESI†). Complex **2** showed complete internalization into the cancer cells within 4 h of incubation, while its slow uptake (∼44%) was observed for normal MCF-10A cells. The results indicate different rates of cellular uptake of the complex into the cancer

Table 1 The IC_{50} (μM) values of the oxovanadium(IV) complexes

	HeLa	MCF-7	MCF-10A
Complex	Light (dark)	Light (dark)	Light (dark)
1	44.1 ± 1.8[a] (59.3 ± 1.7)	53.3 ± 1.9[a] (72.5 ± 2.1)	85.2 ± 1.7[a] (90.2 ± 2.2)
2	0.24 ± 0.02[a] (>40)	0.53 ± 0.03[a] (>40)	>40[a] (>40)

[a] Light of 400–700 nm wavelength. IC_{50} values for acdppz are 9.5 ± 0.3 μM in HeLa; >20 μM for MCF-7 cells in the light. It is >20 μM in the dark. H_2L·HCl gave an IC_{50} of >100 μM under light and dark conditions in all the cell lines used.

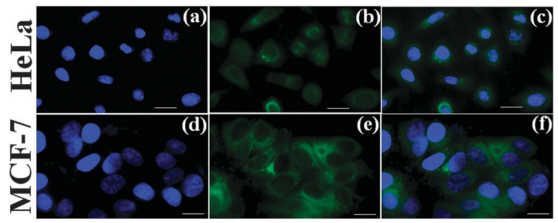

Fig. 4 Fluorescence microscopic images of the HeLa and MCF-7 cancer cells treated with **2** (10 μM) upon 4 h incubation and Hoechst 33342 dye (5 μg ml^{-1}): panels (a, d) show the blue emission of the Hoechst dye staining nucleus; panels (b, e) show green emission of **2**; panels (c, f) are the merged images showing cytosolic localization of **2**. Scale bar = 20 μm.

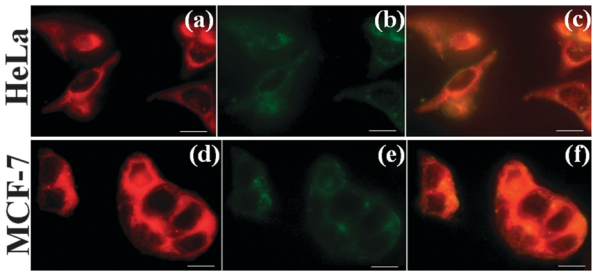

Fig. 5 Fluorescence microscopic images of **2** (10 μM) and ER-tracker red (ERTR, 0.5 μM) in HeLa and MCF-7 cells after 4 h incubation: panels (a, d) show fluorescence of ERTR; panels (b, e) show fluorescence images of **2** and panels (c, f) show the merged images of ERTR and **2**. Scale bar: 20 μm.

versus normal cells, suggesting that the VB6 in the complex is capable of differentiating the cancerous and normal cells with potential to act as a tumour-targeting PDT agent. Complex **2** having acridine as a fluorescent tag was used for the fluorescence microscopy study. A significant cellular uptake of **2** was observed within 2 h and continued up to 4 h (Fig. 4, Fig. S24 and S25 ESI†). Dual staining with nuclear staining dye Hoechst 33342 (blue emission) showed primarily cytosolic localization of **2** within the cells as viewed from the merged images shown in panels (c) and (f) of Fig. 4. This is a novel result as localization of **2** in the nuclei could damage the nuclear DNA leading to possible mutation and carcinogenesis. We probed the specificity of localization of the complex to endoplasmic reticulum (ER) and/or mitochondria. The merged images shown in panels (c) and (f) of Fig. 5 with the ER Tracker Red indicate selective localization of **2** in the ER (Fig. S26 and S27, ESI†). In contrast, studies using mitotracker red showed no apparent mitochondrial localization of **2** (Fig. S28, ESI†). Preliminary result which showed that ~70% of vanadium gets into the ER is of significance since ER stress is well known to increase the ROS production leading to the activation of the apoptotic cascade.[7,13]

In summary, the Schiff base vitamin B6 oxovanadium(IV) complex [VO(HL)(acdppz)]Cl (**2**) having (acridinyl)dipyridophenazine base in a ternary structure showed a remarkable PDT effect in visible light (400–700 nm, 10 J cm^{-2}) specifically targeting the endoplasmic reticulum (ER) of the cancer cells while being less toxic in the dark even after 48 h of incubation and to the normal cells. The VTC-mediated diffusion pathway is found to be operative for the cellular uptake of the complexes. The photocytotoxicity of complex **2** compares well to that of the PDT drug Photofrin®. The localization of **2** in ER and generation of $^1O_2$ as ROS may be responsible for induction of apoptosis in visible light through the trigger of ER stress response. The results showing ER localisation of **2** and the light-induced apoptosis by ERSR are distinctly different from other PDT agents. This work has opened up a new avenue in photo-chemotherapeutics by targeting ER of the cancer cells instead of nuclear or mitochondrial DNA. Further studies are ongoing to understand the mechanistic aspects of the ER-targeted apoptotic cell death.

We thank the DST, Government of India, and the CSIR, New Delhi, for funding (SR/S5/MBD-02/2007; 01(2559)/12/EMR-II/2012); the AvH Foundation, Germany, for an electrochemical system; and Mr S. Mukherjee for his help in computational studies. A.R.C. thanks DST for J.C. Bose fellowship. S.B. thanks the UGC, New Delhi, for a research fellowship.

Notes and references

‡ Crystal data for **1a**·EtOH: $C_{26}H_{27}ClN_4O_9V$, M = 625.91, triclinic, $P\bar{1}$, a = 9.4205(5) Å, b = 11.9369(11) Å, c = 13.5029(11) Å, α = 68.758(8)°, β = 77.535(5)°, γ = 84.902(6)°, U = 1381.80(19) $Å^3$, Z = 2, D_c = 1.504 Mg m^{-3}, T = 293(2) K, reflections collected/unique [R(int)]: 19 241/6319 [0.0412], F(000) = 646, GOOF = 1.036, $R_1[wR_2]$ = 0.0578 [0.1246] for 6319 reflections [$I > 2\sigma(I)$] and 378 parameters [$R_1(F^2)$ = 0.0862 (all data)]. X-ray (Mo-K_α) data from Bruker SMART APEX CCD diffractometer. Structure resolution by SHELX system of programs.[14]

1 (*a*) I. R. Canelon and P. J. Sadler, *Inorg. Chem.*, 2013, **52**, 12276–12291; (*b*) F. S. Mackay, J. A. Woods, P. Heringová, J. Kašpárková, A. M. Pizarro, S. A. Moggach, S. Parsons, V. Brabec and P. J. Sadler, *Proc. Natl. Acad. Sci. U. S. A.*, 2007, **104**, 20743–20748.
2 (*a*) J. J. Wilson and S. J. Lippard, *J. Med. Chem.*, 2012, **55**, 5326–5336; (*b*) G. Y. Park, J. J. Wilson, Y. Song and S. J. Lippard, *Proc. Natl. Acad. Sci. U. S. A.*, 2012, **109**, 11987–11992.
3 (*a*) E. Delaey, F. V. Laar, D. D. Vos, A. Kamuhabwa, P. Jacobs and P. D. Witte, *J. Photochem. Photobiol., B*, 2000, **55**, 27–36; (*b*) J. Saczko, M. Mazurkiewicz, A. Chwilkowska, J. Kulbacka, G. Kramer, M. Ługowski, M. Śnietura and T. Banas, *Folia Biol.*, 2007, **53**, 7–12.
4 (*a*) S. Wu and D. Xing, *J. X-Ray Sci. Technol.*, 2013, **20**, 363–372; (*b*) I. Kinzler, E. Haseroth, C. Hauser and A. Rück, *Photochem. Photobiol. Sci.*, 2007, **6**, 1332–1340.
5 (*a*) S. Marrachea and S. Dhar, *Proc. Natl. Acad. Sci. U. S. A.*, 2012, **109**, 16288–16293; (*b*) S. Marrachea, S. Tundup, D. A. Harn and S. Dhar, *ACS Nano*, 2013, **7**, 7392–7402; (*c*) P. Prasad, I. Khan, P. Kondaiah and A. R. Chakravarty, *Chem. – Eur. J.*, 2013, **19**, 17445–17455.
6 (*a*) S. Shen, Y. Zhang, R. Zhang and X. Gong, *Biochem. Biophys. Res. Commun.*, 2013, **15**, 519–524; (*b*) S. E. Logue, P. Cleary, S. Saveljeva and A. Samali, *Apoptosis*, 2013, **18**, 537–546; (*c*) G. G. Johnson, M. C. White and M. Grimaldi, *Curr. Pharm. Des.*, 2011, **17**, 284–292.
7 (*a*) J. Choi, Y. Lim, S. Cho, J. Lee, J. A. Jeong, E. J. Kim, J. B. Park, S. H. Kim, H. S. Park, H. Kim and C. Song, *Cell Death Dis.*, 2013, **4**, e957, DOI: 10.1038/cddis.2013.489; (*b*) H. Kim, G. Lee, E. Y. Cho, S. Chae, T. Ahn and H. Chae, *J. Cell Sci.*, 2009, **122**, 1126–1133; (*c*) T. Verfaillie, A. D. Garg and P. Agostinis, *Cancer Lett.*, 2013, **332**, 249–264.
8 S. Wang and R. J. Kaufman, *J. Cell Biol.*, 2012, **197**, 857–867.
9 M. Mariappan, M. Suenaga, A. Mukhopadhyay, P. Raghavaiah and B. G. Maiya, *Inorg. Chim. Acta*, 2011, **376**, 340–349.
10 (*a*) S. Pandey, P. Garg, K. T. Lim, J. Kim, Y.-H. Choung, Y.-J. Choi, P.-H. Choung, C.-S. Cho and J. H. Chung, *Biomaterials*, 2013, **34**, 3716–3728; (*b*) J. F. Gregory, *Nutr. Rev.*, 1992, **50**, 295–297; (*c*) H. Hellmann and S. Mooney, *Molecules*, 2010, **15**, 442–459; (*d*) S. B. Renwick, J. V. Skelly, K. J. Chave, P. G. Sanders, K. Snell and U. Baumann, *Acta Crystallogr., Sect. D*, 1998, **54**, 1030–1031.
11 M. J. Frisch, *et al.*, *GAUSSIAN 09*, Gaussian Inc., Wallingford, CT, 2009, see ESI† for complete citation.
12 S. Banerjee, P. Prasad, A. Hussain, I. Khan, P. Kondaiah and A. R. Chakravarty, *Chem. Commun.*, 2012, **48**, 7702–7704.
13 X. Huang, L. Li, L. Zhang, Z. Zhang, X. Wang, X. Zhang, L. Hou and K. Wu, *Br. J. Nutr.*, 2013, **109**, 727–735.
14 G. M. Sheldrick, *SHELX-97, Programs for Crystal Structure Solution and Refinement*, University of Göttingen, Göttingen, Germany, 1997.

